PROCEEDINGS OF SCIENCE

Distinguishing Axion-Like Particles and 2HDM Higgs bosons in $t\bar{t}$ production at the LHC

Anke Biekötter,[a] **Thomas Biekötter,**[b] **Alexander Grohsjean,**[c] **Sven Heinemeyer,**[d] **Laurids Jeppe,**[e,*] **Christian Schwanenberger**[e,c] **and Georg Weiglein**[e,c]

[a] *Johannes Gutenberg-Universität Mainz, Saarstr. 21, 55122 Mainz, Germany*

[b] *Institute for Theoretical Physics, Karlsruhe Institute of Technology, Wolfgang-Gaede-Str. 1, 76131 Karlsruhe, Germany*

[c] *Universität Hamburg, Luruper Chaussee 149, 22761 Hamburg, Germany*

[d] *Instituto de Física Téorica UAM-CSIC, Cantoblanco, 28049, Madrid, Spain*

[e] *Deutsches Elektronen-Synchrotron DESY, Notkestr. 85, 22607 Hamburg, Germany*

E-mail: laurids.jeppe@desy.de

We present an analysis of the sensitivity of LHC searches for new spin-0 particles produced via gluon-fusion and decaying into top-antitop-quark ($t\bar{t}$) final states to generic axion-like particles (ALPs) coupled to top-quarks and gluons. We derive new limits on the effective ALP Lagrangian in the linear representation in terms of the Wilson coefficients c_t and $c_{\tilde{G}}$ based on the existing CMS search using 35 fb^{-1} of proton-proton scattering data collected at $\sqrt{s}$ = 13 TeV. We further investigate posssible distinctions between ALPs and pseudoscalar Higgs bosons as predicted by the Two Higgs doublet model (2HDM), and find that a distinction is possible with data anticipated to be collected during the high-luminosity phase of the LHC for a significant range of the effective ALP-gluon coupling.

The European Physical Society Conference on High Energy Physics (EPS-HEP2023)
21-25 August 2023
Hamburg, Germany

*Speaker

PoS(EPS-HEP2023)474

1. Introduction

Axions and axion-like particles (ALPs, denoted a) are spin-0 particles that are gauge-singlets under the Standard Model (SM) gauge groups. ALPs appear in many well-motivated SM extensions, where they arise as pseudo-Nambu-Goldstone bosons of an approximate axion shift-symmetry. As a consequence, the masses of ALPs can naturally be much smaller than the energy scale of the underlying UV model, making them an attractive target for the Large Hadron Collider (LHC) and the future High-Luminosity LHC (HL-LHC). While axions have originally been introduced as a potential solution to the strong-CP problem [1–3], ALPs are featured in many different SM extensions including supersymmetric theories, dark-matter models and composite Higgs models, see e.g. [4] for a recent review.

In this work, we consider heavy ALPs production in the process $pp \to a \to t\bar{t}$ at the LHC. Recently, the CMS collaboration published the results of a search for heavy additional Higgs bosons in $t\bar{t}$ final states using 35.6 fb^{-1} of data [5]. In this work, we recast this analysis by considering an ALP that couples to top quarks and additionally contains an effective coupling to the gluon field strength. Such an effective coupling to gluons does not exist for a pseudoscalar Higgs boson as contained in models that extend the SM only in the Higgs sector, such as the Two Higgs doublet model (2HDM). By taking an effective ALP-gluon-gluon coupling into account here, we can address the question how a pseudoscalar Higgs boson as predicted in 2HDMs could be distinguished from a more generally defined ALP that may have additional couplings to gluons.

2. Theoretical framework

We assume an ALP that interacts with the SM only via couplings to gluons and the top quark, with other couplings not relevant to our analysis. In this case, the linear ALP-SM Lagrangian is given by

$$\mathcal{L} = \mathcal{L}_{\text{SM}} + \frac{1}{2}(\partial_\mu a)(\partial^\mu a) + \frac{m_a^2}{2}a^2 - \frac{a}{f_a} c_G \, G^a_{\mu\nu}\tilde{G}^{a\mu\nu} - \mathrm{i}c_t \, \frac{a}{f_a}\left(\bar{q}\, Y_t \, \tilde{H}\, t_R + \text{h.c.}\right) , \tag{1}$$

where f_a denotes the ALP scale, Y_t the top-quark Yukawa coupling, t_R is the right-handed top-quark spinor, and the left-handed top- and bottom-quark spinors are contained in the $SU(2)$ doublet $q = (t_L, b_L)^T$. Moreover, H is the Higgs doublet and $G^a_{\mu\nu}$ denotes the gluon field strength tensor. The last part of this Lagrangian directly yields the $at\bar{t}$ vertex in the $pp \to a \to t\bar{t}$ process, with coupling c_t.

For the agg vertex, we need to consider both the direct coupling to the gluons, with coupling strength c_G, and the coupling mediated via a triangle top-quark loop. Integrating out light quark flavors, but keeping the full kinematics of the top quark loop since we consider ALP masses of the same order as the top-quark mass, we arrive at an expression for the effective agg vertex as

$$g^{\text{eff}}_{agg} = 4\pi\frac{c_{\tilde{G}}}{f_a} + \frac{\mathrm{i}}{2}\alpha_s\frac{c_t}{f_a}\left(B_1(\tau) - 1\right) , \tag{2}$$

where $B_1(\tau) = 1 - \tau f^2(\tau)$ is a loop function with

$$f(\tau) = \frac{\pi}{2} + \frac{\mathrm{i}}{2} \ln\left(\frac{1+\sqrt{1-\tau}}{1-\sqrt{1-\tau}}\right) . \tag{3}$$

Since the loop function B_1 is a function of the event kinematics, we expect the distributions of observables for the process $pp \to a \to t\bar{t}$ to be affected by both couplings $c_{\tilde{G}}$ and c_t. One aim of this work was to investigate the effect of these two couplings, as well as the sensitivity to them at the LHC.

It is important to note that in the case $c_{\tilde{G}} = 0$, both the $at\bar{t}$ and agg vertex show exactly the same structure as for an additional pseudoscalar Higgs boson as predicted by e.g. the 2HDM (further denoted as A). As such, for this case, the same shape is expected for kinematic distributions in the two models, and experimental search results for 2HDM Higgs bosons may be directly translated into results for an ALP (see Sec. 4.1 below). On the other hand, for non-vanishing values of $c_{\tilde{G}}$ a distinction between an ALP and a Higgs boson as predicted in multi-Higgs models is possible, as we will discuss in Sec. 4.2.

3. Monte Carlo simulation

We generate Monte Carlo (MC) events of the process $pp \to a/A \to t\bar{t} \to b\bar{b}\ell^+\ell^-\nu\bar{\nu}$ at leading order (LO) in QCD using the general-purpose MC generator MadGraph 5 [6]. Similarly, SM $t\bar{t}$ events are generated at next-to-leading order (NLO) in QCD using the MC generator Powheg [7] in order to estimate the SM background.

Similar to the CMS search for a heavy pseudoscalar Higgs boson [5], we discriminate the signal and background events based on two variables, the invariant mass of the $t\bar{t}$ system $m_{t\bar{t}}$ and the spin correlation variable c_{hel}. The latter is defined as

$$c_{\mathrm{hel}} = \cos\varphi = \hat{\ell}^+ \cdot \hat{\ell}^- , \tag{4}$$

where φ denotes the angle between the directions of flight $\hat{\ell}^+$ and $\hat{\ell}^-$ of the two leptons, defined respectively in the rest frames of their parent top or antitop quarks.

We apply a Gaussian smearing with a standard deviation of $\sigma = 7.5\%$ directly on $m_{t\bar{t}}$ to roughly estimate the finite detector resolution in an experiment. Based on the numbers reported by CMS in Ref. [5], we approximate the experimental acceptances to be 5 % for the signal and 10 % for the $t\bar{t}$ background.

4. Results

4.1 Translation of Higgs limits

Since an ALP and an additional pseudoscalar Higgs boson show the same coupling structure to the top quark as long as $c_{\tilde{G}} = 0$ is assumed for the ALP, any existing limits on the process $pp \to A \to t\bar{t}$ can be directly translated into limits on the ALP coupling to the top quark. Using the definition of c_t as shown in Eq. (1), one finds that the mass- and width-dependent limits on the pseudoscalar Higgs-boson coupling g_{Att} resulting from $A \to t\bar{t}$ searches are equivalent to upper

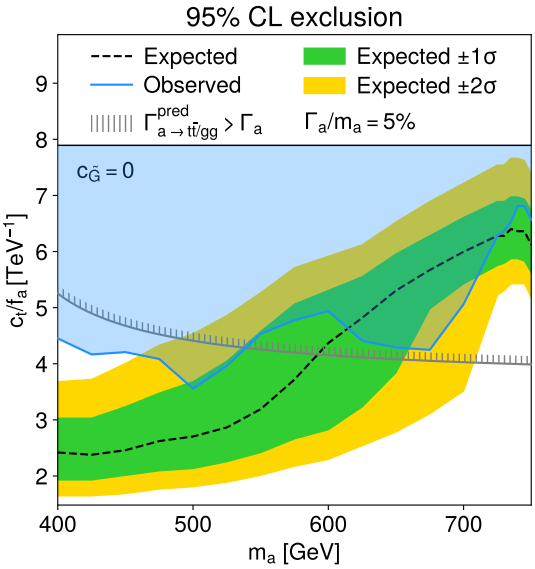

Figure 1: Limit on the coupling of an ALP to the top quark c_t/f_a in the case $c_{\tilde{G}} = 0$, translated from Ref. [5], for a relative ALP width of 5%. The hashed band shows the unphysical region where the total predicted ALP width is larger than the assumed width.

limits on the ALP couplings c_t determined via the relation $c_t/f_a = g_{At\bar{t}}/v$, where $v = 246$ GeV is the SM Higgs vacuum expectation value.

In Fig. 1 we show the expected (black dashed) and observed (blue) upper limits on c_t as a function of the ALP mass assuming a total relative width of 5% based on the results of the CMS search for additional Higgs bosons in $t\bar{t}$ final states using 35.6 fb^{-1} of data [5]. Also shown are the 1σ and 2σ uncertainty bands of the expected limits with the green and yellow bands, respectively.

4.2 Distinguishing between ALPs and pseudoscalar Higgs bosons

Using the MC simulation described in Sec. 3, we estimate the expected difference between SM and BSM prediction for a pseudoscalar Higgs boson as predicted by the 2HDM and for an ALP. In Fig. 2, we show results for several representative values of $c_{\tilde{G}}$ and c_t with signal cross sections of roughly similar order of magnitude as well as the corresponding statistical uncertainties for the integrated luminosity of full LHC Run 2 (138 fb^{-1}). For the pseudoscalar Higgs boson and, equivalently, for an ALP with $c_{\tilde{G}} = 0$, a characteristic peak-dip structure is observed in $m_{t\bar{t}}$ located around the particle mass, which is enhanced compared to the background for high c_{hel}.

For an ALP with $c_{\tilde{G}} \neq 0$, differences in the shape become visible. In particular, when $c_{\tilde{G}}$ and c_t are of opposite sign, the peak-dip might be transformed into a dip-peak instead (e.g. pink line in Fig. 2), or turned into a pure deficit in events (purple line). When $c_{\tilde{G}}$ and c_t have the same sign, the structure is more similar to the $c_{\tilde{G}} = 0$ case but still shows differences in the shapes (e.g. an enhanced peak for the yellow line).

Comparing to the statistical uncertainty (grey band) allows us to estimate whether the differences will be observable: For LHC Run 2, it might already be possible to constrain or observe even relatively small values of $c_{\tilde{G}}/f_a$ for the opposite-sign case, as well as larger values of $c_{\tilde{G}}/f_a$ for

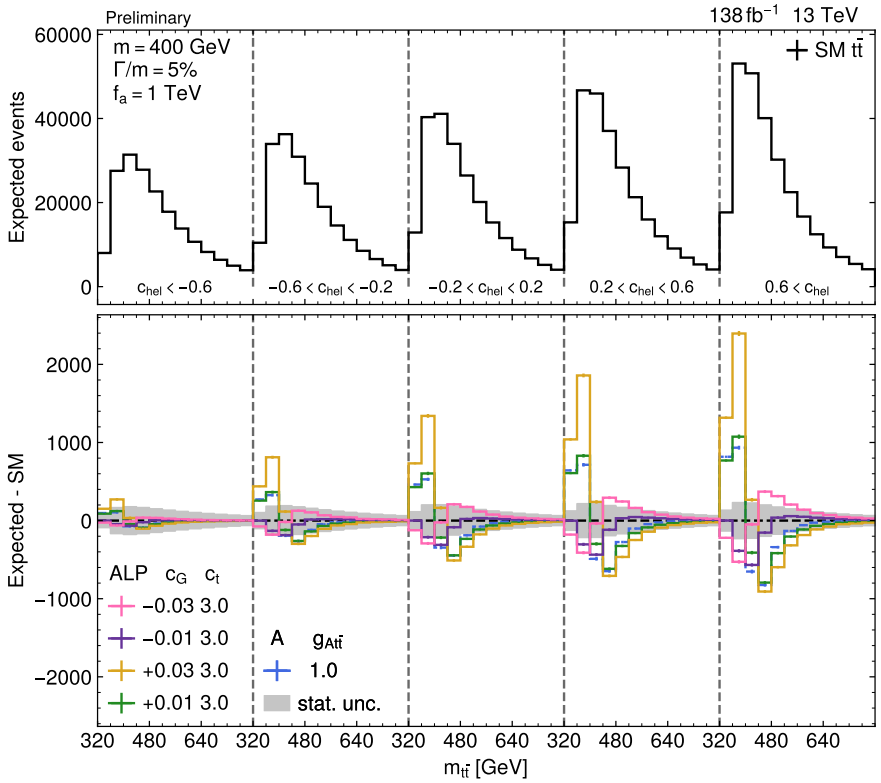

Figure 2: Double-differential distributions in $m_{t\bar{t}}$ and c_{hel} for the SM $t\bar{t}$ background (top panel) as well as an ALP with different values of $c_{\tilde{G}}$ and c_t and a heavy pseudoscalar Higgs boson with $m = 400$ GeV and $\Gamma/m = 5\%$, for an integrated luminosity corresponding to Run 2 (138fb^{-1}). The error bands show the expected statistical uncertainty.

the same-sign case. Going to higher luminosities, tighter constraints can be expected, to the point that at the HL-LHC even very small deviations from the $c_{\tilde{G}} = 0$ case could be detected and a direct measurement of the two couplings could be feasible.

4.3 Projected ALP limits

The increase in data projected to be collected at the LHC Run 3 and especially the HL-LHC will give significant improvements to limits on the ALP couplings $c_{\tilde{G}}$ and c_t. To quantify this, we estimate projected limits for the $a \to t\bar{t}$ final state presented here, similar to Ref. [5].

For this purpose, a hypothesis test based on a binned profile likelihood is performed with the package pyhf [8]. Several sources of systematic uncertainty from theory predictions are included, namely the total rate of the SM $t\bar{t}$ background, taken as a log-normal uncertainty of 4%; the value of the top mass assumed in the simulation of the SM $t\bar{t}$ background, set to $m_t = 172.5$ GeV by default and assigned a Gaussian uncertainty of 1%; missing higher orders in the calculation of both the signal and the $t\bar{t}$ background; and uncertainties in the choice of the parton density function (PDF). For the HL-LHC projection, all systematic uncertainties are halved since the accuracy of theoretical calculations is expected to improve significantly on the relevant timescales.

The projected limits resulting from this procedure can be seen in Fig. 3 for two different ALP masses.

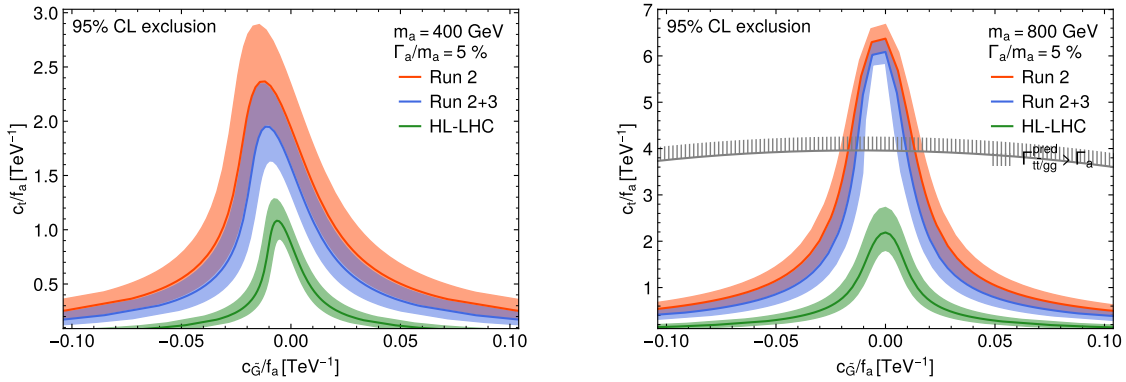

Figure 3: Projected expected limits on the ALP couplings $c_{\tilde{G}}$ and c_t as obtained by the maximum likelihood fit for three different integrated luminosities, corresponding to LHC Run 2 as well as the projections for Run 2+3 and HL-LHC, and for two different ALP masses. In the right plot, the hashed band shows the unphysical region where the total predicted ALP width is larger than the assumed width, while this band would be outside of the displayed c_t range in the left plot.

References

[1] R.D. Peccei and H.R. Quinn, *CP Conservation in the Presence of Instantons*, *Phys. Rev. Lett.* **38** (1977) 1440.

[2] S. Weinberg, *A New Light Boson?*, *Phys. Rev. Lett.* **40** (1978) 223.

[3] F. Wilczek, *Problem of Strong P and T Invariance in the Presence of Instantons*, *Phys. Rev. Lett.* **40** (1978) 279.

[4] K. Choi, S.H. Im and C. Sub Shin, *Recent Progress in the Physics of Axions and Axion-Like Particles*, *Ann. Rev. Nucl. Part. Sci.* **71** (2021) 225 [2012.05029].

[5] CMS collaboration, *Search for heavy Higgs bosons decaying to a top quark pair in proton-proton collisions at $\sqrt{s}$ = 13 TeV*, *JHEP* **04** (2020) 171 [1908.01115].

[6] J. Alwall, R. Frederix, S. Frixione, V. Hirschi, F. Maltoni, O. Mattelaer et al., *The automated computation of tree-level and next-to-leading order differential cross sections, and their matching to parton shower simulations*, *JHEP* **07** (2014) 079 [1405.0301].

[7] S. Alioli, P. Nason, C. Oleari and E. Re, *A general framework for implementing NLO calculations in shower Monte Carlo programs: the POWHEG BOX*, *JHEP* **06** (2010) 043 [1002.2581].

[8] L. Heinrich, M. Feickert, G. Stark and K. Cranmer, *pyhf: pure-Python implementation of HistFactory statistical models*, *Journal of Open Source Software* **6** (2021) 2823.